

LETTER TO THE EDITOR

# NGC 6388 reloaded: some like it hot, but not too much<sup>★</sup>

Eugenio Carretta<sup>1</sup> and Angela Bragaglia<sup>1</sup>

INAF-Osservatorio di Astrofisica e Scienza dello Spazio di Bologna, via Gobetti 93/3, I-40129 Bologna, Italy

## ABSTRACT

Multiple stellar populations in globular clusters (GCs) are defined and recognized by their chemical signature, with second generation stars showing the effects of nucleosynthesis in the more massive stars of the earliest component formed in the first star formation burst. High temperature H-burning produces the whole pattern of (anti)-correlations among proton-capture elements widely found in GCs. However, where this burning occurred is still debated. Here we introduce new powerful diagnostic plots to detect evidence (if any) of products from proton-capture reactions occurring at very high temperatures. To test these Detectors Of High Temperature (in short DOHT) H-burning plots we show how to put stringent constraints on the temperature range of the first generation polluters that contributed to shape the chemistry of multiple stellar population in the massive bulge GC NGC 6388. Using the largest sample to date (185 stars) of giants with detailed abundance ratios in a single GC (except  $\omega$  Cen) we may infer that the central temperature of part of the polluters must have been comprised between  $\sim 100$  and  $\sim 150$  million Kelvin (MK) if we consider hydrostatic H-burning in the core of massive stars. A much narrower range (110 to 120 MK) is inferred if the polluters can be identified in massive asymptotic giant branch (AGB) stars.

**Key words.** Stars: abundances – Stars: atmospheres – Stars: Population II – Galaxy: globular clusters – Galaxy: globular clusters: individual: NGC 6388

## 1. Introduction

The multiple stellar populations in Galactic globular clusters (GCs) are characterized by their pattern of light elements (C, N, O, Na, Mg, Al, Si, and sometime heavier species such as Ca, Sc, and K). One component, which is believed to be the first to be formed in a proto-GC, presents the same level of abundance ratios as the vast majority of metal-poor halo stars at the same metallicity. However, the so called second-generation (SG) shows alterations in the abundances of these elements that range from moderate to extreme. The network of correlations and anti-correlations found among these species represents a key clue to explain the origin of multiple stellar population, since all the observed relations can be traced back to one single mechanism, H-burning.

Since the pioneering studies by Denisenkov and Denisenkova (1989) and Langer et al. (1993) it was clear that proton-capture reactions in H-burning at high temperature could account for all the chemical modifications observed. The enhancement in the abundance ratios of a given element is accompanied (and explained) by the depletion of some other species participating to the network of proton-capture reactions. The uncertainties related to the modeling of stellar structures and to the release of processed material into the intracluster medium hamper at present the knowledge of the exact sites where this burning occurred. Several candidate polluters were proposed, ranging from the less massive ones (intermediate-mass asymptotic giant branch stars, AGB; Cottrell and Da Costa 1981; Ventura et al. 2001) up to supermassive objects (Denisenkov and Hartwik 2014),

passing from fast-rotating massive stars (Decressin et al. 2007) or interacting massive binaries (de Mink et al. 2009).

Fortunately, the variety of nuclear reactions involved in this burning provides some clues, since proton-capture on heavier and heavier nuclei must account for the increasing Coulomb barrier. As a consequence, higher and higher temperatures are required to activate the relevant reactions, which thus provide ideal thermometers to probe the inner structure of the stellar sites where the nucleosynthesis occurred. Thus, fusion temperatures  $\geq 40$  MK are enough for the conversion of O into N and the production of Na from the NeNa cycle to work simultaneously. This rather modest threshold explains why the Na-O anticorrelation is so widespread among GCs that it was proposed to be considered the main signature of the presence of multiple populations, in other words the genuine essence of a globular cluster (Carretta et al. 2010). The higher temperatures ( $\geq 70$  MK) necessary for the MgAl cycle to efficiently operate, apparently are possible only among stars in a subset of GCs, because the Mg-Al anti-correlation was only found in massive and/or metal-poor GCs (Carretta et al. 2009a), as later confirmed by further studies (Mészáros et al. 2015; Pancino et al. 2017; Nataf et al. 2019). These are also the GCs where some overproduction of Si is observed (e.g. Carretta et al. 2009a), pointing out that temperatures in excess of 80-100 MK were attained in the polluters (e.g. Prantzos et al. 2017). Finally, even higher temperatures  $> 100 - 180$  MK (Ventura et al. 2012; Prantzos et al. 2017) are required to explain the Mg-K and Mg-Sc anticorrelations, including some of the heaviest proton-capture species and observed in a couple of peculiar GCs: NGC 2808 (Mucciarelli et al. 2015; Carretta 2015) and NGC 2419 (Mucciarelli et al. 2012; Cohen et al. 2012).

In the present Letter we exploit these different thermometers to design new diagnostic plots that we named Detectors Of High Temperature (DOHT) H-burning products, since they allow to

Send offprint requests to: E. Carretta, eugenio.carretta@inaf.it

<sup>★</sup> Based on observations collected at ESO telescopes under programmes 073.D-0211, 073.D-0760, 381.D-0329, 095.D-0834, and 099.D-0047

reveal the effects (if any) of reactions activated at unusually high temperatures, exceeding the ones typically occurring in the majority of clusters' polluters. We test the DOHT plots by putting strong constraints on the temperature range of the putative polluters that shaped the chemical pattern of multiple populations in the massive GC NGC 6388.

Data and analysis are briefly summarized in Section 2, whereas results are presented in Section 3 and discussed in Section 4.

## 2. The dataset

NGC 6388 is a bulge cluster of high total mass, yet only 37 stars with determined abundances of proton-capture elements were available (Carretta et al. 2007, 2009b), due to the high field contamination affecting this GC. This problem was recently overcome (Carretta and Bragaglia 2018, hereinafter Paper I) by exploiting the large sample of stellar spectra in the cluster region present in the ESO archive as well as newly granted observing time. Here we present results based on homogeneous abundances of Mg, Ca, Sc of more than 180 giants, the largest sample of stars with detailed abundance analysis in a GC (with the notable exception of  $\omega$  Cen). This dataset was used to test the new DOHT plots, as shown in the next Section.

Our results are based on abundances partly from UVES spectra presented in Paper I (23 stars), partly on new UVES spectra (11 stars), and finally on 149 stars with abundances of Fe, Mg, Ca, Sc from GIRAFFE spectra and the high-resolution setup HR13. We acquired new data with the ESO programme 099.D-0047 (PI Carretta) and used archival spectra of three programmes: 381.D-0329(B), PI Lanzoni; 073.D-0760(A), PI Cate-lan; 095.D-0834(A), PI Henault-Brunet, plus the original data from our FLAMES survey (073.D-0211, PI Carretta). The detailed abundance analysis for all stars not presented in Paper I will be described in a forthcoming paper (Carretta and Bragaglia 2019a). However, it closely follows our homogeneous procedures (see Carretta et al. 2009a,b for the UVES and GIRAFFE spectra, respectively) for deriving abundances and estimating star-to-star errors. The metallicity for NGC 6388 is  $[\text{Fe}/\text{H}] = -0.480$  dex (rms=0.045 dex, 35 stars), based on UVES spectra (Carretta and Bragaglia 2019a) and on the same method used to derive the metal abundance for NGC 2808 ( $[\text{Fe}/\text{H}] = -1.129$  dex, rms=0.030 dex, 31 stars, Carretta 2015), that we will use as a comparison in the next Section.

## 3. Temperature range of FG polluters in NGC 6388

The first constraint simply expands over the result already shown in Paper I, and based on abundances from UVES spectra. In Figure 1 we show the Mg-Si anti-correlation in NGC 6388, which is found to be statistically very significant: the Pearson regression coefficient  $r_p$  is -0.48 (34 stars), with a two-tail probability to be a random result  $p = 4.0 \times 10^{-3}$ .

This is clearly due to the well known leakage from Mg-Al cycle on  $^{28}\text{Si}$ : when the  $^{27}\text{Al}(p,\gamma)^{28}\text{Si}$  reaction takes over  $^{27}\text{Al}(p,\alpha)^{24}\text{Mg}$  a certain amount of  $^{28}\text{Si}$  is produced by proton-captures (see Karakas and Lattanzio 2003). This overproduction of Si occurs typically at temperatures  $> 100$  MK, even if the leakage from the Mg-Al cycle already starts at about 65 MK (Arnould et al. 1999). The first constraint then stems from these observations, strengthened and well assessed by the analysis of 11 new red giants with UVES spectra in Carretta and Bragaglia (2019a; red points in Figure 1).

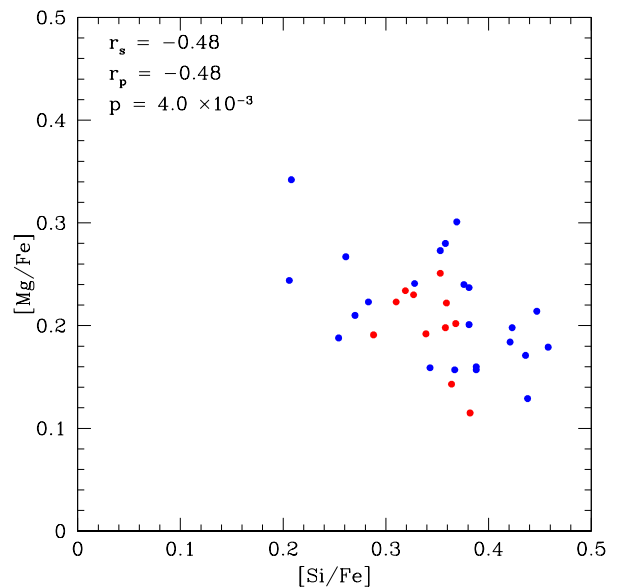


**Fig. 1.** Anti-correlation of  $[\text{Mg}/\text{Fe}]$  and  $[\text{Si}/\text{Fe}]$  abundance ratios in NGC 6388. Blue and red circles indicate stars from Paper I and the new stars analyzed in Carretta and Bragaglia (2019a), respectively. The Spearman rank correlation ( $r_s$ ) coefficient, the Pearson linear correlation ( $r_p$ ) coefficient and its  $p$ -value are listed.

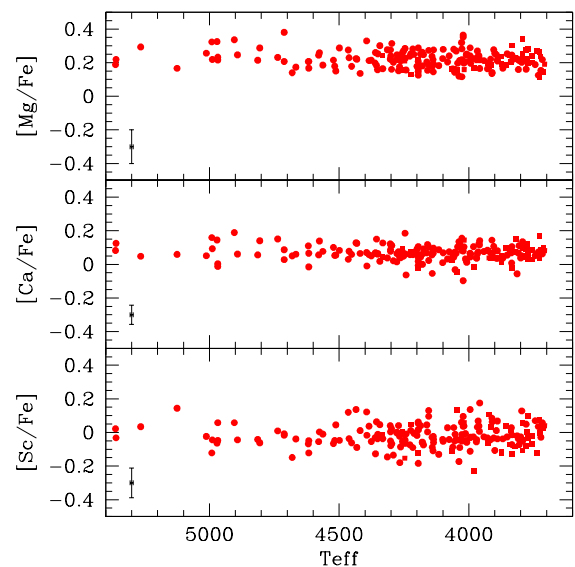


**Fig. 2.** The ratios  $[\text{Mg}/\text{Fe}]$  (184 stars),  $[\text{Ca}/\text{Fe}]$ , and  $[\text{Sc}/\text{Fe}]$  (185 stars) from FLAMES spectra in NGC 6388 (Carretta and Bragaglia 2019a) as a function of effective temperature. Internal error bars are shown in each panel.

A second limit to the temperature range in FG polluters active at the cluster formation may be provided by looking at the abundances of Mg, Ca, and Sc, available for 184, 185, and 185 stars, respectively, in NGC 6388 (Carretta and Bragaglia 2019a). The abundance ratios are plotted in Figure 2 as a function of the effective temperatures. Star to star error bars are also shown and estimated (as described in Carretta et al. 2009b as 0.100 dex, 0.057 dex, and 0.088 dex for  $[\text{Mg}/\text{Fe}]$ ,  $[\text{Ca}/\text{Fe}]$ , and  $[\text{Sc}/\text{Fe}]$ , respectively).

The constraint on the H-burning temperature in the stellar sites that forged the proton-capture elements ending up in forming the multiple populations in NGC 6388 may be fully appreciated from the two panels in Figure 3, that we name DOHT plots. In this Figure we used field stars from Gratton et al. (2003) as reference, since the majority of the field stars only show the chemical pattern derived from the Supernovae (SNe) nucleosynthesis, with no trace of the peculiar proton-capture nucleosynthesis which is restricted to the dense environment of GCs (e.g. Gratton et al. 2000; Smith and Martell 2003).

The distribution of stars of NGC 6388 (red points) in the Ca-Mg and Sc-Mg planes matches almost perfectly that of field stars: Ca and Sc abundances in this GC are not modified by the action of proton-capture reactions.

Conversely, the observations present a different scenario in NGC 2808, a GC slightly less massive than NGC 6388 (total absolute magnitude  $M_V = -9.39$  and  $M_V = -9.41$  mag, respectively: Harris 1996, on-line version 2010). The same abundances are plotted (green triangles) in the two panels of Figure 3 and all elemental ratios are obtained with extremely homogeneous procedures, the same adopted also for NGC 6388. The pattern observable in NGC 2808 is strikingly different, with abundances of both Ca and Sc being anti-correlated to abundances of Mg. Both these relations are found to be statistically very significant (Carretta 2015). This behaviour was attributed to the same process of proton-capture at very high temperature (above 100 MK) postulated to act in GCs like NGC 2419 to produce potassium from proton capture on  $^{36}\text{Ar}$  nuclei (Ventura et al. 2012). The observations in NGC 2808 are explained with this high temperature process, where the formation of proton-rich species is shifted toward heavier nuclei. The effect are obviously more marked on Sc (and K) than Ca, the latter being much more abundant.

The inference for the case of NGC 6388 is straightforward: the H-burning in the FG polluters in this GC was not able to reach temperatures high enough to substantially modify the abundances of Ca and Sc with respect to the levels from SNe nucleosynthesis.

#### 4. Discussion and conclusions

Summarizing the observational evidence found in NGC 6388, we notice (i) overproduction of Si likely due to the increased leakage from the Mg-Al cycle (Paper I and the present letter, Figure 1), and (ii) absence of significant Ca-Mg and Sc-Mg anti-correlations in the new diagnostic plot introduced in the present work (Figure 3).

Prantzos et al. (2017) made extensive H-burning nucleosynthesis calculations in the range of temperature and density suitable to hydrostatic burning in the H-shell of AGB stars or in the cores of massive and supermassive stars. After accounting for the minimum dilution factor required to reproduce the most extreme O abundances in NGC 2808, they found that a limited temperature range (70-80 MK) is able to reproduce all the extreme observed values of O, Na, Mg, and Al in this cluster. The high extreme of this range also accounts for the observed Si abundances in NGC 2808. Only the burning temperature required for K production exceeds this range, since the extreme K abundances in NGC 2808 only are reproduced for  $T \sim 180$  MK. A similar discussion can be found in D'Antona et al. (2016).

In NGC 6388 we do not have (yet) determinations of  $[\text{K}/\text{Fe}]$ , but we can address the production of the heavy proton-capture elements by looking at Ca and Sc, with similar atomic numbers, whose abundances are also clearly altered by H-burning in FG polluters of NGC 2808 (Carretta 2015). At odds with the latter

case, in the present study we found from the DOHT plots that in NGC 6388 the distribution of Ca and Sc closely follows that of field stars at similar metallicity. Conversely, we see robust evidence that Si is altered (Paper I for the GIRAFFE sample and Carretta and Bragaglia 2019a for the GIRAFFE sample), implying temperatures higher than 100 MK. Since heavier elements (like Ar and K) do not start to be affected by nuclear burning before  $T \sim 150$  MK (Prantzos et al. 2017), our present results allow to pinpoint a rather limited range of temperature ( $\sim 100 - 150$  MK) where the H-burning in the putative FG polluters occurred. An even narrower range can be estimated if the polluters can be identified in massive AGB stars. In Figure 1 of D'Antona et al. (2016), at metallicities corresponding to that of NGC 6388, the maximum temperature  $T_{HBB}$  at the bottom of the convective envelope for masses evolving in AGB exceeds the one necessary to produce Si, but never reaches the one required to process Ar into K or heavier species. In this case a range 110-120 MK may explain the observed abundances in NGC 6388.

However, already with the limited sample of stars available in Paper I there was some hints that a single source of pollution is probably not enough to fit all the multi-elements observations with a dilution model in NGC 6388. More stringent conclusions will be drawn when the full set of light elements (O, Na, Mg, Al, Si, with Ca and Sc as the heaviest extreme) will be available.

The present Letter highlights an application to infer the temperature range at which past polluters were active and illustrates how much precise could be the constraints potentially available from large samples with a complete set of homogeneous abundances of proton-capture elements from spectroscopy. The new diagnostic DOHT plots seem to be a powerful tool to test the existence of products from nuclear processing at very high temperatures. The GCs where this very advanced H-burning operated are currently rare, but their census is growing. Among these GCs we may already annoverate NGC 2808 (Carretta 2015), NGC 2419 (Mucciarelli et al. 2012; Cohen et al. 2012), and NGC 4833 (Carretta and Bragaglia 2019b).

Datasets like the one used here and in the forthcoming paper can be used by theoreticians to test and tune both models and derived scenarios up to moderately high metal abundances. A set of calculations for NGC 6388, like those presented by D'Antona et al. (2016) and Prantzos et al. (2017) for NGC 2808 and Prantzos et al. (2007) for NGC 6752, would be very welcome, especially because the abundances in all these three GCs, spanning 1 dex in  $[\text{Fe}/\text{H}]$ , are obtained in a very homogeneous way.

*Acknowledgements.* We thank Raffaele Gratton for useful discussions. This research has made use of the services of the ESO Science Archive Facility, of the SIMBAD database (in particular Vizier), operated at CDS, Strasbourg, France, and of the NASA's Astrophysical Data System.

#### References

- Arnould, M., Goriely, S., Jorissen, A. 1999, *A&A*, 347, 572
- Carretta, E. 2015, *ApJ*, 810, 148
- Carretta, E., Bragaglia, A. 2018, *A&A*, A614, A109 (Paper I)
- Carretta, E., Bragaglia, A. 2019a, in preparation
- Carretta, E., Bragaglia, A. 2019b, in preparation
- Carretta, E., Bragaglia, A., Gratton, R.G. et al. 2007, *A&A*, 464, 967
- Carretta, E., Bragaglia, A., Gratton, R.G., Lucatello, S. 2009a, *A&A*, 505, 139
- Carretta, E., Bragaglia, A., Gratton, R.G. et al. 2009b, *A&A*, 505, 117
- Carretta, E., Bragaglia, A., Gratton, R.G. et al. 2010, *A&A*, 516, 55
- Cohen, J.G., Kirby, E.N. 2012, *ApJ*, 760, 86
- Cottrell, P.L., Da Costa, G.S. 1981, *ApJ*, 245, L79
- D'Antona, F., Vesperini, E., D'Ercole, A. et al. 2016, *MNRAS*, 458, 2122
- de Mink, S.E., Pols, O.R., Langer, N., Izzard, R.G. 2009, *A&A*, 507, L1
- Decressin, T., Meynet, G., Charbonnel, C., et al. 2007, *A&A*, 464, 1029

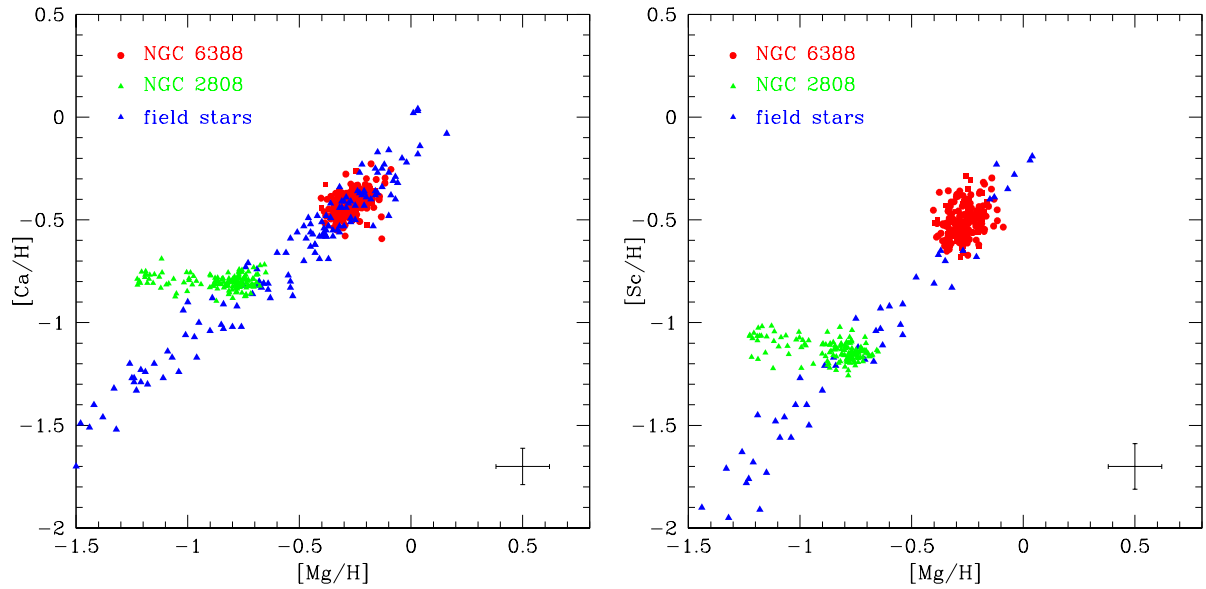


**Fig. 3.** The ratios  $[Ca/H]$  (left panel) and  $[Sc/H]$  (right panel) as a function of  $[Mg/H]$  for giants in NGC 6388 (red points), superimposed to field stars from Gratton et al. (2003; blue triangles). Green triangles are giants in NGC 2808 from Carretta (2015). Internal star-to-star errors refer to NGC 6388.

- Denisenkov, P.A., & Denisenkova, S.N. 1989, *Astr. Zh.*, 1538, 11  
 Denisenkov, P.A., Hartwick, F.D.A. 2014, *MNRAS*, 437, L21  
 Gratton, R.G., Carretta, E., Claudi, R., Lucatello, S., & Barbieri, M. 2003, *A&A*, 404, 187  
 Gratton, R.G., Sneden, C., Carretta, E., Bragaglia, A. 2000, *A&A*, 354, 169  
 Harris, W. E. 1996, *AJ*, 112, 1487  
 Karakas, A.I., Lattanzio, J.C. 2003, *PASA*, 20, 279  
 Langer, G.E., Hoffman, R., & Sneden, C. 1993, *PASP*, 105, 301  
 Mészáros, S., Martell, S.L., Shetrone, M. et al. 2015, *AJ*, 149, 153  
 Mucciarelli, A., Bellazzini, M., Ibata, R. et al. 2012, *MNRAS*, 426, 2889  
 Mucciarelli, A., Bellazzini, M., Merle, T., Plez, B., Dalessandro, E., Ibata, R. 2015, *ApJ*, 801, 68  
 Nataf, D.M., Wyse, R., Schiavon, R.P. et al. 2019, arXiv:1904.07884  
 Pancino, E., Romano, D., Tang, B. et al. 2017, *A&A*, 601, A112  
 Prantzos, N., Charbonnel, C., Iliadis, C. 2007, *A&A*, 470, 179  
 Prantzos, N., Charbonnel, C., Iliadis, C. 2017, *A&A*, 608, A28  
 Smith, G.H., Martell, S.L. 2003, *PASP*, 115, 1211  
 Ventura, P., D'Antona, F., Mazzitelli, I., Gratton, R. 2001, *ApJ*, 550, L65  
 Ventura, P., D'Antona, F., Di Criscienzo, M., Carini, R., D'Ercole, A., Vesperini, E. 2012, *ApJ*, 761, L30